## Research on the Operation Plan of Multi-level Rail Transit Across Lines

Shuoyue Gao, Changfeng Zhu, Yunqi Fu, Jie Wang, Linna Cheng, and Rongjie Kuang

Abstract—Cross-line Operation (CO) of multi-level rail transit achieves resource sharing, complementarity, and promotes inter-level connectivity. Traditional transfer modes often struggle to meet cross-line passenger demand during peak hours. To address this problem, this paper constructs a passenger travel behavior choice model based on prospect theory and the nested Logit model (PT-NL). This model describes passenger decision-making mechanisms influenced by multiple attributes, including time, cost, and comfort. Decision variables, such as train operation frequency and turnback station location, are established. The optimization model incorporates constraints like passenger flow demand, departure frequency, and turnback capacity. Its objectives are minimizing passenger travel time and enterprise operating costs. Results show that compared to the transfer connection mode, the CO mode reduces cross-line passenger travel time by an average of 35.8 minutes. Furthermore, total passenger travel time decreases by 70.00%, and total enterprise operating costs drop by 66.87%. Additional analysis reveals a positive correlation between passengers' time value and their probability of choosing cross-line trains. High-time-value passenger groups show greater sensitivity to direct services, increasing their preference for cross-line trains. The proportion of rigid passenger flow impacts the optimization effectiveness of cross-line train departure frequency. When this proportion exceeds 0.6, the benefit of adding more cross-line trains gradually weakens. Based on these findings, a time-segmented differentiated scheduling strategy is proposed. This strategy prioritizes adding cross-line trains during periods dominated by rigid passenger flow. Conversely, during flexible passenger flow scenarios, frequency can be moderately reduced to optimize costs. This study provides theoretical support for the collaborative optimization of multi-level rail transit networks.

Index Terms—Cross-line operation; Operation Plan; PT-NL; Passenger flow distribution; NSGA-II

Manuscript received May 21, 2025; revised August 21, 2025.

This work was supported in part by the National Natural Science Foundation of China (No.72161024) and "Double-First Class" Major Research Programs, Educational Department of Gansu Province (No.GSSYLXM-04).

Shuoyue Gao is a postgraduate student at School of Traffic and Transportation, Lanzhou Jiaotong University, Lanzhou 730070, China. (e-mail: 18049395600@163.com).

Changfeng Zhu is a professor at School of Traffic and Transportation, Lanzhou Jiaotong University, Lanzhou 730070 China (Corresponding author, phone: +86 189 1989 1566, e-mail: cfzhu003@163.com).

Yunqi Fu is a doctoral candidate at School of Traffic and Transportation, Lanzhou Jiaotong University, Lanzhou 730070, China. (e-mail: 13240002@stu.lzjtu.edu.cn).

Jie Wang is a doctoral candidate at School of Traffic and Transportation, Lanzhou Jiaotong University, Lanzhou 730070, China. (e-mail: 1009696615@qq.com).

Linna Cheng is a doctoral candidate at School of Traffic and Transportation, Lanzhou Jiaotong University, Lanzhou 730070, China. (e-mail: chengjj @163.com).

Rongjie Kuang is a doctoral candidate at School of Traffic and Transportation, Lanzhou Jiaotong University, Lanzhou 730070, China. (e-mail: kuangrj@126.com).

### I. INTRODUCTION

RBANIAZTION continues to advance rapidly, and urban populations are expanding significantly. This trend has spurred regional coordinated development as a key strategy [1]. Within urban agglomerations and metropolitan areas, Multi-level Rail Transit Networks (MRTNs) have emerged as a primary driver for developing interconnected urban clusters [2]. MRTNs integrate various rail transit types. Unlike traditional single-level networks, MRTNs offer greater flexibility to adjust capacity. This flexibility helps meet passengers' diverse travel demands.

However, coordinating multiple rail transit levels within MRTNs presents challenges. The high demands of operational organization increase the complexity of connecting and transferring between different modes [3]. Furthermore, as urban agglomerations grow and commuting distances extend, traditional transfer connection modes often fail to meet passenger needs, especially during peak hours. To address this, scholars have proposed the Cross-line Operation (CO) model [4]. This model aims to achieve functional complementarity and resource sharing across different rail transit levels. Crucially, CO breaks through traditional organizational boundaries. It enables seamless operation of trains across different standards. Existing research on CO primarily focuses on three key areas:

First, studies address the connection problem within MRTNs. Considerable research exists on the spatial layout of rail transit hubs and transfer systems. This theoretical foundation is relatively mature. Research on transfer connection modes mainly concentrates on two aspects: transfer operation modes and transfer node location selection. For instance, Guo Dongbo et al. [5] tackled passenger transfer issues in same-platform scenarios. They proposed coordinated optimization of train schedules across multiple rail transit lines. Bandera and Lemer S [6], along with Saffarzadeh [7], investigated optimal airport transfer hub shapes. Their goal was minimizing passenger transfer walking distances, providing valuable insights for rail transit hubs. Regarding node selection, Eiichi Taniguchi, Michihiko Noritake et al. [8] optimized rail transit network design and transfer node placement.

Despite this progress, existing transfer connection modes increasingly struggle to meet passenger demands as urbanization intensifies. Consequently, research has shifted towards the CO model. On CO feasibility, Peng Qiyuan et al. [9] identified five coordination models for regional multi-standard rail transit. They explored suitable models for different development stages. Wang Meng et al. [10] detailed key technologies for intercity trains crossing into metro lines. They also analyzed core CO implementation technologies.

Second, research tackles the construction of cross-line operation plans. Numerous scholars have examined operation schemes under CO conditions. For example, TANG et al. [11], [12] developed two mixed integer linear programming models. These models addressed cross-line train scheduling with and without capacity constraints. Yang et al. [13], [14] proposed a mixed integer nonlinear programming (MINLP) model. This model explored the benefits of cross-line express trains. Tang et al. [15] built an optimization model for cross-line train operation schemes from station classification and passenger flow allocation perspectives. Building on this, some researchers investigated co-optimizing cross-line operation with other factors using nonlinear models. Li et al. [16] created a MINLP model for co-optimizing train operation plans and stop times in cross-line mode. Chen et al. [17] considered dynamic passenger flow influence. They proposed a nonlinear model to minimize total train deviation and enhance passenger service quality. Shao et al. [18] developed an integrated optimization model. This model combined cross-line train schedules and stop schemes while considering resource allocation fairness.

Third, studies focus on passenger travel choice behavior. As research advances, experts increasingly examine passenger choice behavior. Discrete choice models, particularly the MNL model, and expected utility models are widely used. For example, Xuan Di et al. [19] reviewed literature related to bounded rationality. Ma Shuhong [20] modeled passenger choice behavior by constructing a service train topological network. Yao Enjian et al. [21] developed a route selection model based on disaggregate theory. They introduced the concept of a transfer threshold.

However, these studies typically assume passengers are fully rational decision-makers. In reality, passenger travel decisions are influenced by personal experiences, social factors, and economic conditions. Passengers cannot perceive decision-making information, exhibiting bounded rationality characteristics. Therefore, many scholars have turned to Prospect Theory (PT) and Cumulative Prospect Theory (CPT). For instance, Li Xiaojing et al. [22] proposed a CPT-based commuter route choice model featuring two reference points. Li Ying et al. [23] developed a peak-hour commuter transfer behavior decision model using CPT. Han Baoming et al. [24] defined a generalized time cost calculation based on travel time and cost. They constructed a passenger route choice model using the PT-NL (Prospect Theory-Nested Logit) framework. Key value and weight functions are summarized in Table 1.

Although prior research contributes to multi-level rail transit network optimization, most work concentrates on

transfer connection modes. Further investigation into the CO model is lacking. Some studies on cross-line operation schemes exist, but they often assume complete passenger rationality. They also frequently overlook passengers' multi-attribute choice behavior characteristics. To address these gaps, this paper makes the following contributions:

- (i) We developed a passenger travel choice behavior model based on PT-NL. PT captures passengers' choice behavior under bounded rationality when selecting different trains. NL determines the probabilities of passengers choosing different travel modes.
- (ii) We established a multi-objective cross-line operation train scheme model. This model incorporates varying passenger time values. It minimizes passenger travel costs and enterprise total costs. Key constraints include passenger flow demand, train occupancy rates, departure frequencies, and turnaround station capacities.
- (iii) We designed a non-dominated sorting genetic algorithm. This algorithm rapidly screens non-dominated solutions. It then employs fuzzy logic to select the ideal solution. We also improved the traditional NSGA-II algorithm to obtain the optimal strategy set.

The remainder of this paper is structured as follows: Section 2 analyzes passenger travel choice behavior under bounded rationality. Section 3 constructs the cross-line train operation plan model. Section 4 details the non-dominated sorting genetic algorithm. Section 5 presents a case study. Finally, Section 6 concludes the article.

#### II. PROBLEM DESCRIPTION

Consider a multi-level rail transit network denoted as  $\Omega = \{TN \mid TN_1, TN_2\}$ . This network contains two interconnected lines, denoted as  $\Gamma = \{L \mid L_S, L_R\}$ . The set of stations along these lines is  $x = \{x_i \mid x_1, x_2, ..., x_n\}$ . Within this set,  $\{x_1, x_2, ..., x_a, ..., x_m\}$  represents stations belonging to line  $L_S$ , and  $\{x_m, ..., x_b, ..., x_n\}$  represents stations belonging to line  $L_R$ . These two lines physically connect at station  $x_m$ .

During peak hours, significant cross-line passenger flow occurs between the different lines. Passengers traveling across lines need to transfer at station  $x_m$ . To mitigate the inconvenience caused by transfers for both passengers and operators, cross-line trains are operated. These trains run directly between station  $x_a$  on line  $L_{\mathcal{S}}$  and station  $x_b$  on line

 $L_R$ . A schematic diagram of the lines is shown in Fig.1.

TABLE I SUMMARY OF VALUE FUNCTIONS AND WEIGHT FUNCTIONS

Value function		Weight function		
Name	Expressions	Name	Expressions	
Linear	v(x) = x	Linear	$\pi(p) = p$	
Logarithmic	$v(x) = \ln(a+x)$	Power	$\pi(p) = p^{\gamma}$	
Power	$v(x) = x^a$	Goldstein-Einhorn	$\pi(p) = sp^{\gamma} / (sp^{\gamma} + (1 - p^{\gamma}))$	
Quadratic	$v(x) = ax + bx^2$	Tversky-Kahneman	$\pi(p) = p^{\gamma} / (p^{\gamma} + (1-p)^{\gamma})^{\gamma}$	
Bell	$v(x) = bx - e^{-ax}$	Prelec I	$\pi(p) = e^{-(\ln(p))^{\gamma}}$	
HARA	$v(x) = -(b+x)^a$	Prelec II	$\pi(p) = e^{-s(\ln(p))^{\gamma}}$	

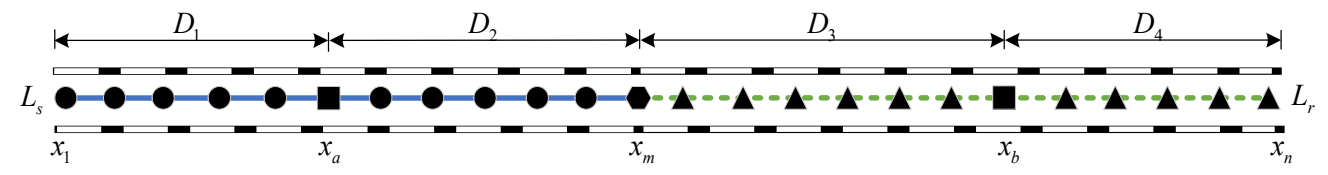


Fig.1. Problem Description Diagram

Trains are categorized into two types: local trains and cross-line trains. A local train operates solely within a single section of either line  $L_S$  or line  $L_R$ . A cross-line train operates across both lines. We denote the local train on line  $L_S$  as S, the cross-line train as G, and the local train on line  $L_R$  as R. The formation sets for these three train types are  $B = \{B_j \mid B_1, B_2, B_3\}$ . Their operating frequency sets are  $F = \{f_k \mid f_1, f_2, f_3\}$ . All three train types follow an all-stop pattern.

Based on the routing of these three train types, the lines are divided into 4 sections:  $D_1$ ,  $D_2$ ,  $D_3$ , and  $D_4$ . Specifically,  $D_1 = [1, a)$ ,  $D_2 = [a, m)$ ,  $D_3 = [m, b)$ , and  $D_4 = [b, n)$ .

### III. MODEL CONSTRUCTION

#### A. Problem Assumptions

- (1) Assuming the passenger flow is stable and passengers can transfer at most once, without considering the situation of passenger congestion;
- (2) Assuming that within the scope of the study, the direction of passenger departure, the nature of the origin and destination points, and the OD passenger flow between stations remain unchanged;
- (3) Assuming all trains stop at stations, with a single route, fixed formation, and the same turnaround time.

#### B. Constraint Analysis

(1) Flow Conservation Constraint. To meet the passenger demand  $Q_{ij}$  for each OD pair, the sum of the passenger volumes allocated to all feasible travel modes must equal this demand.

$$\sum_{h \subset H} q_{ij}^h = Q_{ij} \tag{1}$$

Where,  $Q_{ij}$  represents the total passenger flow volume from station i to station j.

- (2) Passenger Demand Constraint. The transport capacity provided by trains operating on any section must satisfy the total passenger demand on that section.
- 1) In section  $D_1 = [x_1, x_a)$ . Only local train S of line  $L_s$  operates. Therefore, the transport capacity of local train S on line  $L_s$  must satisfy the maximum cross-section passenger flow demand in this section.

$$\sum_{\substack{i=1\\k \neq k}}^{k} \sum_{j=k+1}^{n} q_{ij} \le \beta_s E_{s1} f_1$$
 (2)

2) In section  $D_2 = [x_a, x_m)$ . Both local train S of line  $L_s$  and cross-line train G operate. Therefore, the combined capacity of local train S and cross-line train G must satisfy the maximum cross-section passenger flow demand in this section.

$$\sum_{\substack{i=1\\s \in k < m}}^{k} \sum_{j=k+1}^{n} q_{ij} \le \beta_s (E_{s1} f_1 + E_{s2} f_2)$$
 (3)

3) In section  $D_3 = [x_m, x_b]$ . Local train S of line  $L_s$ ,

cross-line train G, and local train R of line  $L_r$  operate. Therefore, the combined capacity of local train S, cross-line train G, and local train R of line  $L_r$  must satisfy the maximum cross-section passenger flow demand in this section.

$$\sum_{\substack{i=1\\m\leq k < h}}^{k} \sum_{j=k+1}^{n} q_{ij} \le \beta_s (E_{s1} f_1 + E_{s2} f_2) + \beta_r E_{r3} f_3 \qquad (4)$$

4) In section  $D_4 = [x_b, x_n]$ . Local train S of line  $L_r$ , cross-line train G, and local train R of line  $L_r$  operate. Therefore, the combined capacity of local train S, cross-line train G, and local train R of line  $L_r$  must satisfy the maximum cross-section passenger flow demand in this section.

$$\sum_{\substack{i=1\\k < k < n}}^{k} \sum_{j=k+1}^{n} q_{ij} \le \beta_s (E_{s1} f_1 + E_{s2} f_2) + \beta_r E_{r3} f_3 \qquad (5)$$

where:  $\beta_s$  and  $\beta_r$  represent the load factors for train S and train R, respectively;  $E_{si}$  (i=1,2) represent the fixed passenger capacities (persons) of train S and the cross-line train G, respectively;  $E_{r3}$  represents the fixed passenger capacity (persons) of train R.

- (3) Departure Frequency Constraint. To ensure operational service levels, the departure frequency on each line must meet specific requirements. For lines  $L_s$  and  $L_r$ , the combined frequencies of operating trains must satisfy the minimum headway constraint. Additionally, considering that passenger waiting times should not be excessive, the sum of the frequencies of the two train types must not fall below the minimum departure frequency for the line.
- 1) For line  $L_s$ . Both local train S and cross-line train G operate. The sum of their frequencies must not exceed the line capacity  $N_s^{cap}$  of line  $L_s$ . Furthermore, to prevent excessively long passenger waiting times, the sum of their frequencies must not fall below the minimum departure frequency for line  $L_s$ .

$$f_{\text{Smin}} \le f_1 + f_2 \le N_{\text{S}}^{\text{cap}} \tag{6}$$

2) For line  $L_r$ . Both local train R and cross-line train G operate. The sum of their frequencies must not exceed the line capacity  $N_r^{cap}$  of line  $L_r$ . Furthermore, to prevent excessively long passenger waiting times, the sum of their frequencies must not fall below the minimum departure frequency for line  $L_r$ .

$$f_{\rm Rmin} \le f_2 + f_3 \le N_{\rm R}^{\rm Cap} \tag{7}$$

where:  $N_{\rm S}^{\rm cap}$  and  $N_{\rm R}^{\rm cap}$  represent the line capacities of line  $L_{\rm s}$  and line  $L_{\rm r}$ , respectively;  $f_{\rm Smin}$  and  $f_{\rm Rmin}$  represent the minimum departure frequencies for line  $L_{\rm s}$  and line  $L_{\rm r}$ , respectively.

(4) Operating Vehicle Quantity Constraint. To prevent excessively high operating costs, the number of vehicles put into operation must satisfy certain conditions. That is:

$$\max\{\left[\frac{L_{1}+t_{zh}\cdot V_{e}}{60\cdot V_{e}}\right]f_{1}B_{1}, \left[\frac{L_{21}}{60\cdot V_{e}}\right]f_{2}B_{2}\} \leq B_{\max}$$
 (8)

1) Within routing range [1,m]. Both local train S and cross-line train G operate. The maximum number of operating train S and train G must not exceed the maximum number of vehicle utilization  $B_{\max}$ .

$$\max \left\{ \left[ \frac{(L_{21}/V_e) + t_{zh}}{60} \right] f_1 B_1, \left[ \frac{(L_2/V_e) + t_{zh}}{60} \right] f_2 B_2, \\ \left[ \frac{((L_{22}/V_e) + t_{zh})}{60} \right] f_3 B_3 \right\} \leq B_{\max}$$
(9)

2) Within routing range [a,b]. Local trains S and R, as well as cross-line train G, operate. The maximum number of operating trains (all three types) must not exceed the maximum number of vehicle utilization  $B_{\max}$ .

$$\max\{\left[\frac{L_3 + t_{zh}}{60 \cdot V_e}\right] f_3 B_3, \left[\frac{L_{22} + t_{zh} \cdot V_e}{60 \cdot V_e}\right] f_2 B_2\} \le B_{\max} \quad (10)$$

where:  $L_1, L_2, L_3$  represent the routing range lengths (km) of local train S, cross-line train G, and local train R, respectively;  $L_{21}, L_{22}$  represent the routing range lengths (km) of [a,m] and [m,b], respectively;  $B_{\max}$  represents the maximum number of vehicle utilization (units);  $V_e$  represents the train operating speed (km/h);  $\lceil \cdot \rceil$  denotes the ceiling function (rounding up).

(5) Turn-back Station Capacity Constraint. To prevent frequent turn-back operations of cross-line trains at the turn-back station, a limit is imposed on their departure frequency. That is

$$f_2 \le \left\lceil \frac{60}{t_{zh}} \right\rceil, f_2 \in Z^+, \forall f_i \in [f_{\min}, f_{\max}]$$
 (11)

where:  $t_{zh}$  represents the train turn-back time.

To mitigate the impact of frequent cross-line train turn-backs on the capacity of the cross-line section, a minimum over-track section length N must be ensured. That is

$$N \le a + b \le N + n \tag{12}$$

where: N denotes the ceiling function (rounding up); A is determined based on specific line conditions.

(6) Cross-line Routing Range Constraint. To ensure cross-line trains turn back at appropriate stations, the location of the turn-back station must be constrained. That is

$$1 < a < m < b < n \quad \{a, m, b, n \in N^+\}$$
 (13)

(7) Variable integer constraint

$$f_1, f_2, f_3, a, b \in Z^+$$
 (14)

C. Objective Function Analysis

(1) Analysis of Passenger Travel Time

Passenger travel time includes in-vehicle time  $T_{\rm d}$ , waiting time  $T_{\rm w}$ , and transfer time  $T_{\rm z}$ . Waiting time  $T_{\rm w}$  is expressed as

$$T_{\rm w} = \frac{1}{2} \cdot \frac{60}{f_{\nu}} = \frac{30}{f_{\nu}}, \quad \nu = \{1, 2, 3\}$$
 (15)

Where,  $f_{\nu}$  represents the departure frequency of the train;  $f_{1}$ ,  $f_{2}$ ,  $f_{3}$  respectively represent the operating

frequencies (in pairs h) of the train S, the cross-line train G, and the train R.

Considering all trains operate under a station-stop pattern with unchanged parameters, in-vehicle time  $T_d$  remains constant. Therefore, only waiting time and transfer time are considered. Transfer time includes transfer walking time  $w_i$  and transfer waiting time  $e_i$ . Transfer time  $T_z$  is expressed as

$$T_{z} = \tau(e_{i} + w_{i}) \quad \forall a < i < b \tag{16}$$

Where,  $\tau$  is the transfer penalty coefficient, describing physical exertion during transfers.

To account for differences in passengers' time value, a cost conversion weight  $\xi$  is introduced to convert travel expenses into time. The total passenger travel time T is

$$T = \min(\sum_{o=1}^{4} \sum_{o=1}^{4} (T_{od,w} + T_{od,z}) + \xi \cdot (a \cdot q \cdot z_{od} / x))$$
 (17)

Where,  $T_{od, \rm w}$  and  $T_{od, \rm z}$  denote the waiting time and transfer time for passengers traveling from zone o to zone d;  $T_{od}$  represents the travel time from zone o to zone d;  $\xi$  is the cost conversion weight, reflecting passengers' sensitivity differences to travel time and costs, set according to income and trip purpose; a is the daily working hours; q is the statutory working days;  $t_{od}$  indicates the travel cost from zone  $t_{od}$ 0 to zone  $t_{od}$ 1 is the annual per capita income.

Assume a set of travel modes  $H = \{h \mid be, cr\}$ , where cr and be denote passengers choosing cross-line trains and local-line trains, respectively. Considering passengers' travel choices are influenced by factors such as time and cost, passengers' time value vot(h) is introduced to convert time to cost. The generalized travel time  $u_{od}^h$  for choosing travel mode h between interval o and interval d is

$$u_{od}^{h} = (T_{od,w}^{h} + T_{z}) \cdot vot(h) + z_{od}^{h}$$
 (18)

Where,  $z_{od}^h$  is the monetary cost (yuan) of choosing travel mode h between interval o and interval d; vot(h) is the time value coefficient (yuan/min) for mode h.

Considering the bounded rationality of passengers' travel choices, prospect theory is introduced to characterize the choice probability. Passengers' travel types are divided into rigid travel and flexible travel. A penalty coefficient  $\wp$  is introduced to characterize the time value of rigid travelers. Under flexible travel conditions, the travel time value function  $v(u_{od}^h)$  for passengers choosing mode h from zone o to zone d is

$$v(u_{od}^{h}) = \begin{cases} (u_{od}^{o} - u_{od}^{h})^{\alpha} &, u_{od}^{o} \ge u_{od}^{h} \\ -\chi (u_{od}^{h} - u_{od}^{o})^{\beta} - 60 \cdot \psi, u_{od}^{o} < u_{od}^{h} \end{cases}$$
(19)

Where,  $\alpha$  is the gain sensitivity coefficient  $0 \le \alpha \le 1$ ;  $\beta$  is the loss sensitivity coefficient  $0 \le \beta \le 1$ ;  $\psi$  is a 0-1 variable (1 if the passenger's travel type is rigid, otherwise 0);  $u_{od}^{o}$  is the reference point for travel time.

Let the proportion  $\eta_{od}^h$  of passenger flow choosing travel mode h between zone o and zone d to the total flow serve as the actual probability in the weight function. The decision function  $\omega(\eta_{od}^h)$  considering passenger behavior is

$$\omega(\eta_{od}^h) = \frac{\sigma(\eta_{od}^h)^{\rho}}{(1 - \eta_{od}^h)^{\rho} + \sigma(\eta_{od}^h)^{\rho}}, \rho > 1$$
 (20)

Where,  $\sigma$  is the discrimination parameter;  $\rho$  is the attractiveness parameter.

The probability  $P_{od}^h$  of passengers choosing travel mode h from zone o to zone d is

$$P_{od}^{h} = \frac{\exp((U(u_{od}^{h})\omega(\eta_{od}^{h}))/\theta)}{\sum_{h}^{H} \exp((U(u_{od}^{h})\omega(\eta_{od}^{h}))/\theta)}$$
(21)

Where,  $\theta$  indicates the correlation between travel modes, valued in [0,1].

Passenger travel types are classified as direct flow I, transfer flow II, and mixed flow III. The travel times for these three flow types I,II,III are as follows:

Direct flow I has only direct routes. The origin-destination zones are  $[D_1, D_1]$ ,  $[D_2, D_2]$ ,  $[D_3, D_3]$  and  $[D_4, D_4]$ . Direct flow I is shown in Fig.2.

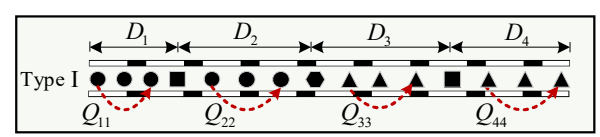


Fig.2. Passenger Flow of Type ]

 $T_{33}$ ,  $T_{22}$ , and  $T_{44}$  are respectively

$$T_{11} = \sum_{i=1}^{a-2} \sum_{j=i+1}^{a-1} q_{ij} \cdot \frac{30}{f_1}$$
 (22)

$$T_{22} = \sum_{i=a}^{m-2} \sum_{j=i+1}^{m-1} q_{ij} \left( p_{22}^{be} \cdot \frac{30}{f_1} + p_{22}^{cr} \cdot \frac{30}{f_2} \right)$$
 (23)

$$T_{33} = \sum_{i=m}^{b-2} \sum_{j=i+1}^{b-1} q_{ij} \left( p_{33}^{cr} \frac{30}{f_2} + p_{33}^{be} \frac{30}{f_3} \right)$$
 (24)

$$T_{44} = \sum_{i=b}^{n-1} \sum_{j=i+1}^{n} q_{ij} \cdot \frac{30}{f_3}$$
 (25)

Transfer flow II requires transfers. The origin-destination zones are  $[D_1, D_3]$ ,  $[D_1, D_4]$ ,  $[D_2, D_4]$  Transfer flow II is shown in Fig.3.

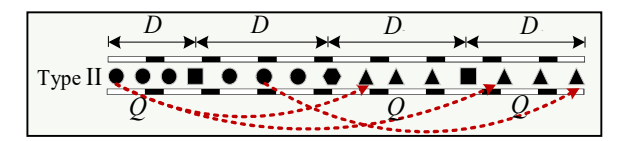


Fig.3. Passenger Flow of type II

 $T_{14}$ ,  $T_{13}$ ,  $T_{24}$  are respectively

$$T_{13} = \sum_{i=1}^{a-1} \sum_{j=m}^{b-1} q_{ij} \left( p_{13}^{be} \left( \frac{30}{f_1} + \frac{30}{f_3} \right) + p_{13}^{cr} \left( \frac{30}{f_1} + \frac{30}{f_2} \right) \right) + T_z$$
 (23)

$$T_{14} = \sum_{i=1}^{a-1} \sum_{j=b}^{n} q_{ij} \cdot \left( \left( \frac{30}{f_z} + \frac{30}{f_z} \right) + T_z \right)$$
 (24)

$$T_{24} = \sum_{i=a}^{m-1} \sum_{j=b}^{n} q_{ij} \left( p_{24}^{cr} \left( \frac{30}{f_2} + \frac{30}{f_3} \right) + p_{24}^{be} \left( \frac{30}{f_1} + \frac{30}{f_3} \right) \right) + T_z$$
 (25)

Mixed flow III has both direct and transfer options with at most one transfer. The origin-destination zones are  $[D_1, D_2]$ ,  $[D_2, D_3]$ , and  $[D_3, D_4]$ . Mixed flow III is shown in Fig.4.

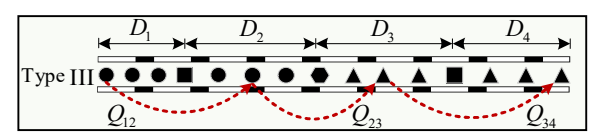


Fig.4. Passenger Flow of type III

 $T_{23}$ ,  $T_{12}$ ,  $T_{34}$  are respectively

$$T_{12} = \sum_{i=1}^{a-1} \sum_{j=a}^{m-1} q_{ij} (P_{12}^{cr} \cdot (\frac{30}{f_1} + \frac{30}{f_2}) + T_z) + P_{12}^{be} \cdot \frac{30}{f_1})$$
 (26)

$$T_{23} = \sum_{i=a}^{m-1} \sum_{i=m}^{b-1} q_{ij} \left( P_{23}^{be} \cdot \left( \frac{30}{f_1} + \frac{30}{f_3} \right) + T_z \right) + P_{23}^{cr} \cdot \frac{30}{f_2} \right)$$
 (27)

$$T_{34} = \sum_{i=m}^{b-1} \sum_{j=b}^{n} q_{ij} (P_{34}^{cr} \cdot (\frac{30}{f_2} + \frac{30}{f_3}) + T_z) + P_{34}^{be} \cdot \frac{30}{f_3})$$
 (28)

## (2) Enterprise operating cost function

Transportation enterprise costs are divided into fixed costs and variable costs. Fixed costs consider only vehicle purchase costs and depreciation costs. Variable costs include expenses related to train operation volume. The fixed costs  $Z_{\rm sc}$  and  $Z_{\rm rc}$  for lines  $L_{\rm S}$  and  $L_{\rm R}$  are respectively:

$$Z_{sc} = (f_1 B_1 T_1 + f_2 B_2 T_2) C_s \tag{29}$$

$$Z_{rr} = f_3 B_3 T_3 C_r (30)$$

Where,  $B_1$ ,  $B_2$ ,  $B_3$  denote the fixed formation sizes (cars) of the three train types;  $T_1$ ,  $T_2$ ,  $T_3$  represent the turnaround times of the three train types;  $C_s$  and  $C_r$  indicate the fixed vehicle costs per unit time (yuan) on lines  $L_s$  and  $L_r$ .

Turnaround time includes running time, dwell time, and turnback time. The turnaround times  $T_1$ ,  $T_2$ , and  $T_3$  for the three train types are:

$$T_k = \frac{\left(\sum_{i=1}^{m-1} t_i^{run} + \sum_{i=2}^{m-1} t_i^{stop}\right)}{3600} + \frac{t_{turn}}{60}, (k = 1, 2, 3)$$
 (31)

Where,  $t_i^{\text{run}}$  is the running time (s) in section [i,i+1];  $t_i^{\text{stop}}$  is the dwell time (s) at station i;  $t_{num}$  is the turnback time (min) at turnback stations.

The variable cost of trains is related to the number of kilometers traveled and the number of running pairs. The operating cost per unit kilometer of trains running on this line is calculated according to the standards of this line. Cross line trains are calculated according to the standards of this line  $L_s$  or  $L_r$  within the scope of this line, and after crossing the line, they are calculated according to the standards of the line they cross. Therefore, the variable costs  $Z_{\rm se}$  and  $Z_{\rm re}$  of the line  $L_s$  and  $L_r$  are respectively

$$Z_{\text{se}} = f_1 B_1 e_s \sum_{i=1}^{m-1} L_i + f_2 B_2 e_s \sum_{i=0}^{m-1} L_i + f_2 B_2 e_r \sum_{i=m}^{b-1} L_i$$
 (32)

$$Z_{re} = f_3 B_3 e_r \sum_{i=m}^{n-1} L_i$$
 (33)

Where,  $e_s$  and  $e_r$  are the system operating costs per car-kilometer (yuan/car-km) on lines  $L_s$  and  $L_r$ ;  $L_i$  is the station spacing (km) for section [i, i+1].

The total cost Z of the transportation enterprise is expressed as

$$Z = Z_{se} + Z_{re} + Z_{sc} + Z_{rc}$$
 (34)

In summary, the dual objectives are to minimize total enterprise operating cost(Z1) and passenger travel time (Z2). That is:

In summary, the objective functions are to minimize the total operating cost of the enterprise Z1 and minimize the travel time of passengers Z2. approach

$$Z1 = \min Z = (Z_{re} + Z_{rc} + Z_{se} + Z_{sc})$$
 (35)

$$Z2 = \min T = \min(\sum_{o=1}^{4} \sum_{d=1}^{4} T_{od} + \xi \cdot (a \cdot q \cdot z_{od} / x))$$
 (36)

#### IV. ALGORITHM DESIGN

The cross-line train operation plan model is a large-scale integer programming problem, and the computational complexity increases with the increase of the number of stations on the line. Based on the constructed cross line operation plan model, an improved Non dominated Sorting Genetic Algorithm (NSGA-II) is designed to optimize the model. Compared with traditional genetic algorithms, NSGA-II can efficiently obtain the Pareto optimal solution set for multi-objective optimization problems in a single run through non dominated sorting and diversity preservation mechanisms, overcoming the single objective limitations of traditional genetic algorithms.

## A. Algorithm steps

Step 1: Chromosome encoding and population initialization. Each set of chromosomes corresponds to a development plan, and the decision variables of the model  $f_1, f_2, f_3, a, b$  jointly participate in chromosome encoding. Based on the characteristics of decision variables, this article adopts dual chromosome binary encoding. The first chromosome carries the frequency information of train operation at once, while the second chromosome carries the range information of cross line intervals. The location of the turnaround station is determined by analyzing the encoding of the second chromosome. The schematic diagram of chromosome encoding is shown in Fig. 5.

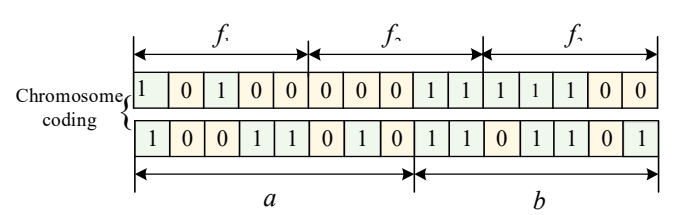


Fig.5. Schematic diagram of chromosome encoding

Step 2: Fitness calculation. Directly using the objective function as the fitness function.

Step 3: Fast non dominated sorting and crowding sorting.

Using travel time cost and enterprise operating cost as fitness functions, calculate the fitness value corresponding to each individual, and stratify the population based on dominance relationships. The first layer is the optimal solution set of the existing population, which is the Pareto boundary. The next layer is a fast non dominated sorting, as shown in Fig.6.

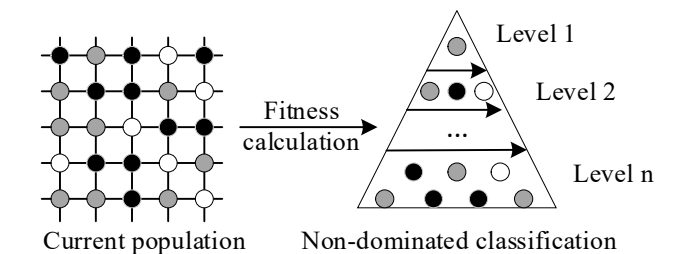


Fig.6. Schematic diagram of non dominated sorting

Step 4: Use crowding algorithm instead of fitness value in genetic algorithm to make the Pareto front as evenly distributed as possible, ensuring population diversity and forming a population  $P_c$ . The c crowding degree of an individual refers to the c distance between two adjacent individuals in the target space.

$$L[c]_d = L[c]_d + \frac{L[c+1]_m - L[c-1]_m}{Z_m^{\max} - Z_m^{\min}}$$
(37)

Where,  $Z_m^{\max}$ ,  $Z_m^{\min}$  represent the m maximum and minimum values of the objective function value at the same level;  $L[c]_d$  represent s the c crowding level of an individual, with an initial value of 0;  $L[c+1]_m$  represents the m value c+1 of the individual's 2th objective function;  $L[c-1]_m$  Represents the m value c-1 of the individual's objective function.

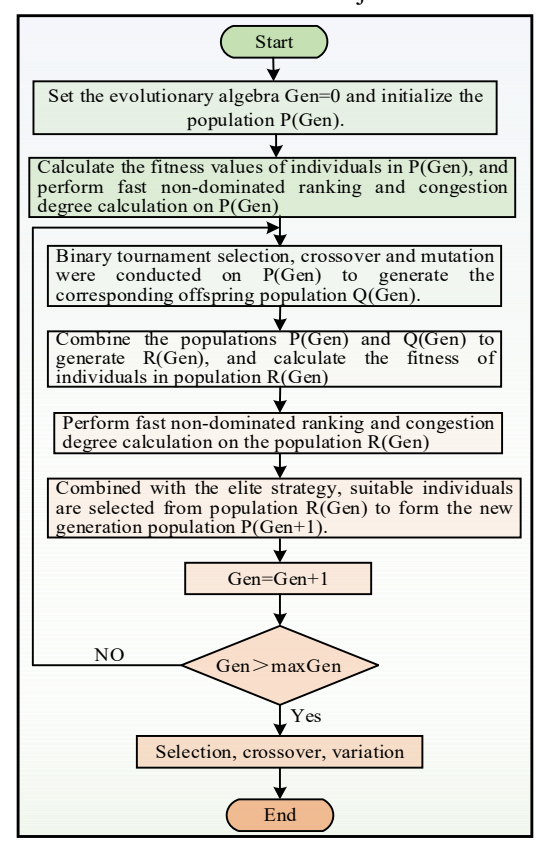


Fig.7. NSGA-II algorithm flowchart

Step 5: Genetic manipulation.

According to the elite selection strategy, the excellent individuals from the parent generation are directly placed in the offspring to prevent them from being lost in mutation crossover and improve the accuracy of optimization results. New offspring populations are generated through selection, crossover, mutation, and other operations until the end condition is met, and genetic operations are stopped to retain the non-dominated solution set of the Pareto front.

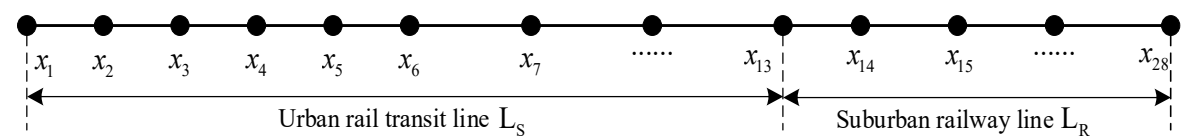


Fig.8. Schematic diagram of cross line operation line

Step 6: Ideal solution screening method. Using fuzzy logic methods to screen ideal solutions.

Firstly, calculate the *i* evaluation values of each candidate solution under the target  $\mu_i$ :

$$\mu_{i} = \begin{cases} 0, & Z_{i}^{\max} \leq Z_{i} \\ \frac{Z_{i} - Z_{i}^{\min}}{Z_{i}^{\max} - Z_{i}^{\min}}, & Z_{i}^{\min} \leq Z_{i} \leq Z_{i}^{\max} \\ 1, & Z_{i} \leq Z_{i}^{\min} \end{cases}$$

$$(38)$$

$$Z_{i}^{\min}, Z_{i}^{\max} \text{ represents the } i \text{ maximum and minimum}$$

Where,  $Z_i^{\min}$ ,  $Z_i^{\max}$  represents the *i* maximum and minimum values of the objective function value of the candidate solution in the Pareto solution set.

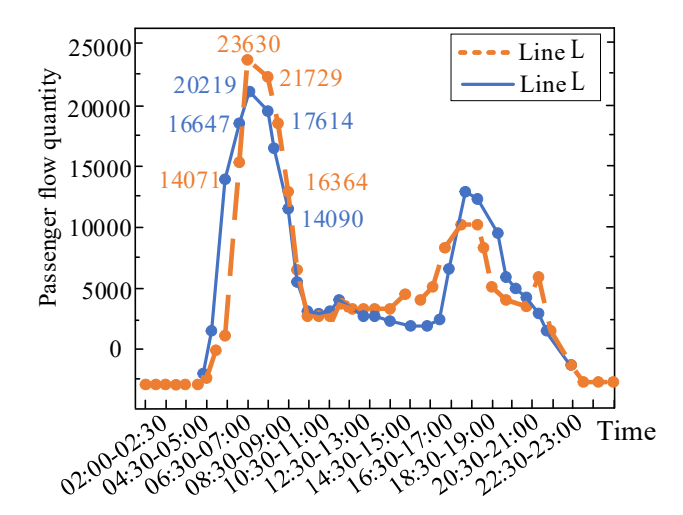
Finally, the k evaluation value of the candidate solution in the Pareto solution set is calculated based on the target evaluation value  $\mu[k]$ . The higher the evaluation value, the more ideal the corresponding candidate solution is.

$$\mu[k] = \sum_{i=1}^{M} \mu_i[k] / \sum_{j=1}^{Npareto} \sum_{i=1}^{M} \mu_i[j]$$
 (39)

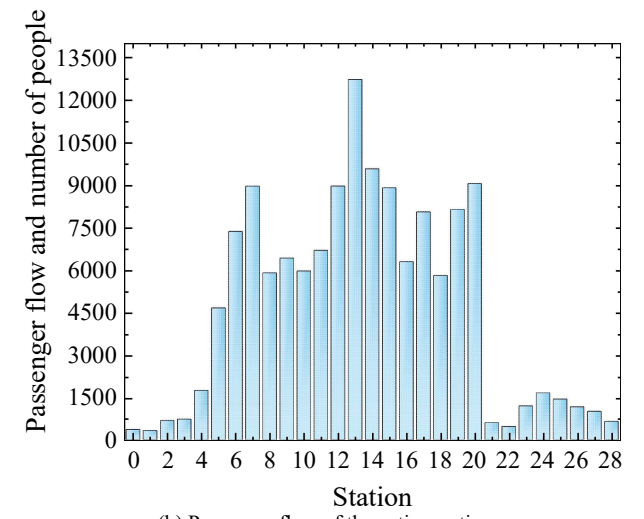
Where, M represents the target number;  $N_{pareto}$  represents the number of k solutions i in the Pareto solution set, and  $\mu_i[k]$  represents the evaluation value of the candidate solution for the 2th objective. The NSGA-II algorithm flow is shown in Fig 7.

## V. CASE STUDY

There are 13 stations on a certain urban rail transit line  $L_s$  and 16 stations on a suburban railway line  $L_R$ . The subway stations and suburban railway stations are combined  $S = \{x_1, x_2, ..., x_{13}\}$  and  $R = \{x_{13}, x_{14}, ..., x_{27}, x_{28}\}$ , the urban rail transit line and suburban railway line  $x_{13}$  operate across lines through junction stations. The per capita disposable income of citizens is x = 81800 yuan/person, the working hours for one day are  $a = 480 \,\mathrm{min}$ , the statutory working days q = 250d, and the penalty for passengers who are late for rigid travel is yuan B = 300,  $\xi = 1$ . The parameters of the weight function under profit conditions  $\delta = 0.72$ ,  $\rho=1.19$ ; In the case of loss  $\delta = 0.76$ ,  $\rho = 1.21$ , the time attribute conversion parameters  $\mathcal{G}_{u}^{hr} = 0.7$  , congestion attribute conversion parameters  $\mathcal{G}_{c}^{hf} = 0.3$ , the formation of different types of trains  $B_{s1} = B_{s2} = B_r = 7$ , the fixed capacity of trains is 1460 people, the full load rate  $\beta_r = \beta_s = 0.8$ , the turnaround time of trains at turnaround stations  $t_{\text{turn}} = 4 \,\text{min}$ , the minimum turnaround time interval  $t_{zh} = 2 \min$ , and the passenger transfer time  $T_h = 0.5 \,\mathrm{min}$ travel  $L_{\rm S} = 32\,{\rm km}$  ,  $L_{\rm R} = 28\,{\rm km}$  . Selecting the research time as peak hours, the analysis of long-term peak hour passenger flow data is shown in Fig.8. The schematic diagram of the cross line operation route is shown in Fig.9.



(a) Full day cross-sectional passenger flow



(b) Passenger flow of the entire section Fig.9. Analysis of Long term Peak Hour Passenger Flow Data

As shown in Fig 9, the distribution of inbound passenger flow time throughout the day follows a unimodal pattern, with significant morning peak characteristics. The  $L_{\rm S}$  morning peak period of the line is  $L_{\rm R}$  about 6:30-9:00, and the morning peak period of the line is about 7:00-9:00. The selected study time is 7:00-8:00.

### A. Model solution results

Use the Python 3.9.13 programming platform to solve the problem, where the parameters of the NSGA-II algorithm are: population size M = 200, external storage quantity N = 100.

The performance of the improved NSGA-II algorithm was compared with that of the traditional Genetic Algorithm (GA) and the traditional NSGA-II algorithm. The comparison of algorithm performance is shown in the table below.

Table 2 Algorithm Performance Comparison

		<u> </u>	
Metric	GA	Traditional NSGA-II	Improved NSGA-II
Z2	28.4	8.3	8.1
<b>Z</b> 1	12.9	12.1	12.9
Number of non-dominated solutions	1	22	38
Convergence generation	300	500	350
Constraint violation rate	41%	15%	0%
Computation time (s)	120	380	420

The iteration curves of the three algorithms are shown in Fig.11.

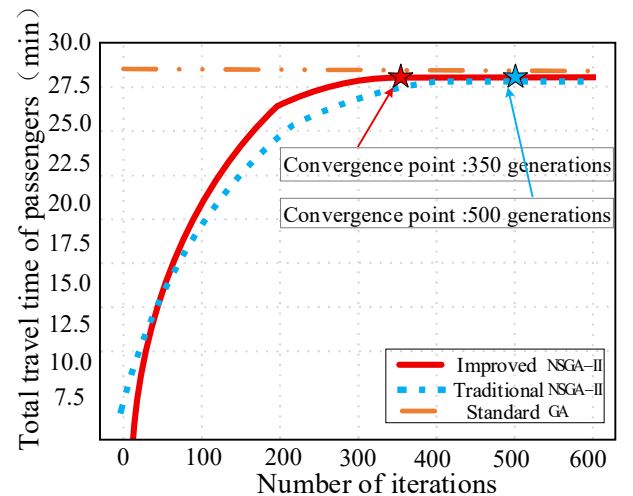
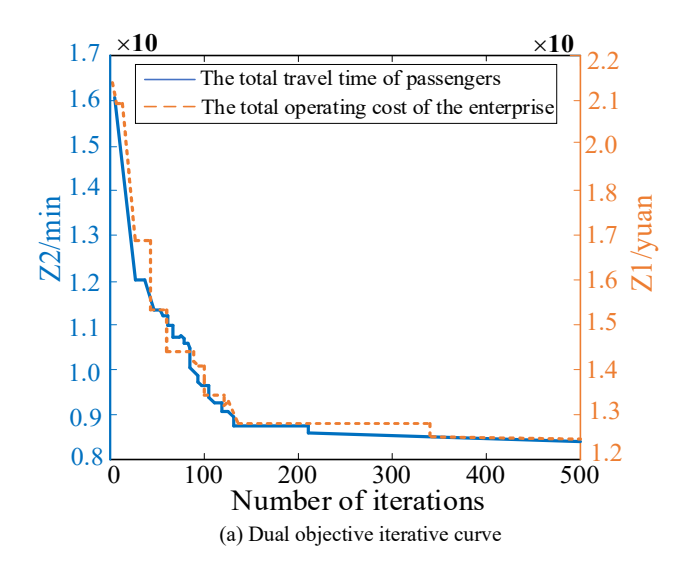


Fig.11. The iteration curves of the three algorithms

As can be seen from Fig 11, the improved algorithm is significantly superior to the traditional algorithms. Comparatively, the improved algorithm converges faster, achieving convergence at 350 generations with a higher quality solution set. It obtains 38 non-dominated solutions, far more than both the traditional and classical algorithms, and exhibits stronger constraint satisfaction capability. Although the computation time is slightly higher than that of the traditional algorithm, it is exchanged for higher solution set quality and constraint satisfaction capability. Therefore, the effectiveness of the designed non-dominated sorting genetic algorithm is validated. The dual objective curve and Pareto front set are shown in Fig.12.



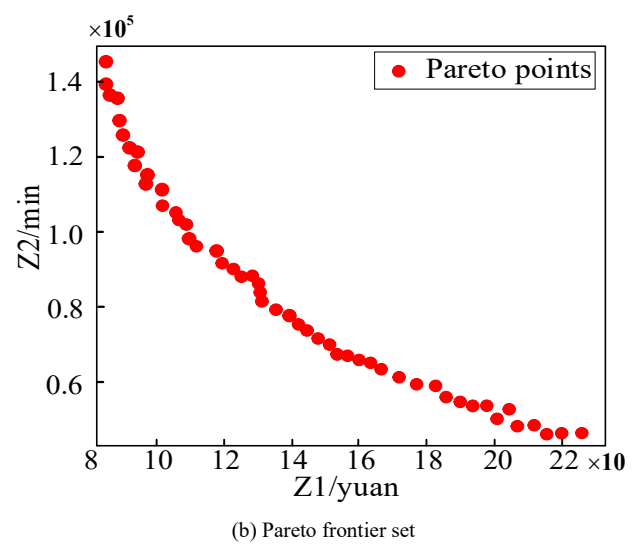


Fig.12. Dual objective iteration curve with Pareto front set

As can be seen from Fig 12, the bi-objective values converge at 350 generations. As the total passenger travel time increases, the total cost of the enterprise gradually decreases, showing a negative correlation.

The enterprise total cost optimal solution, intermediate solution, and passenger travel time optimal solution were selected separately to further analyze the Pareto front. The Pareto images corresponding to these three special solutions are shown in Fig 13. The corresponding specific train operation plans are shown in Fig 14(a), 14(b), and 14(c) respectively. The optimal solution is shown in Fig 15.

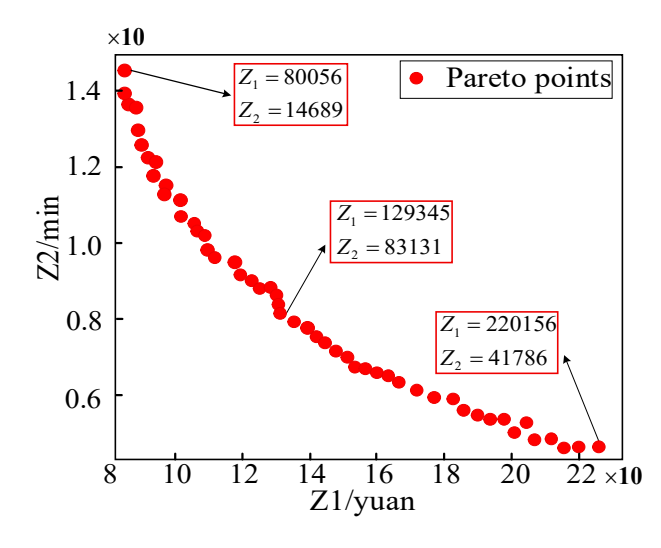


Fig.13. shows the pareto frontier sets corresponding to the three special solutions

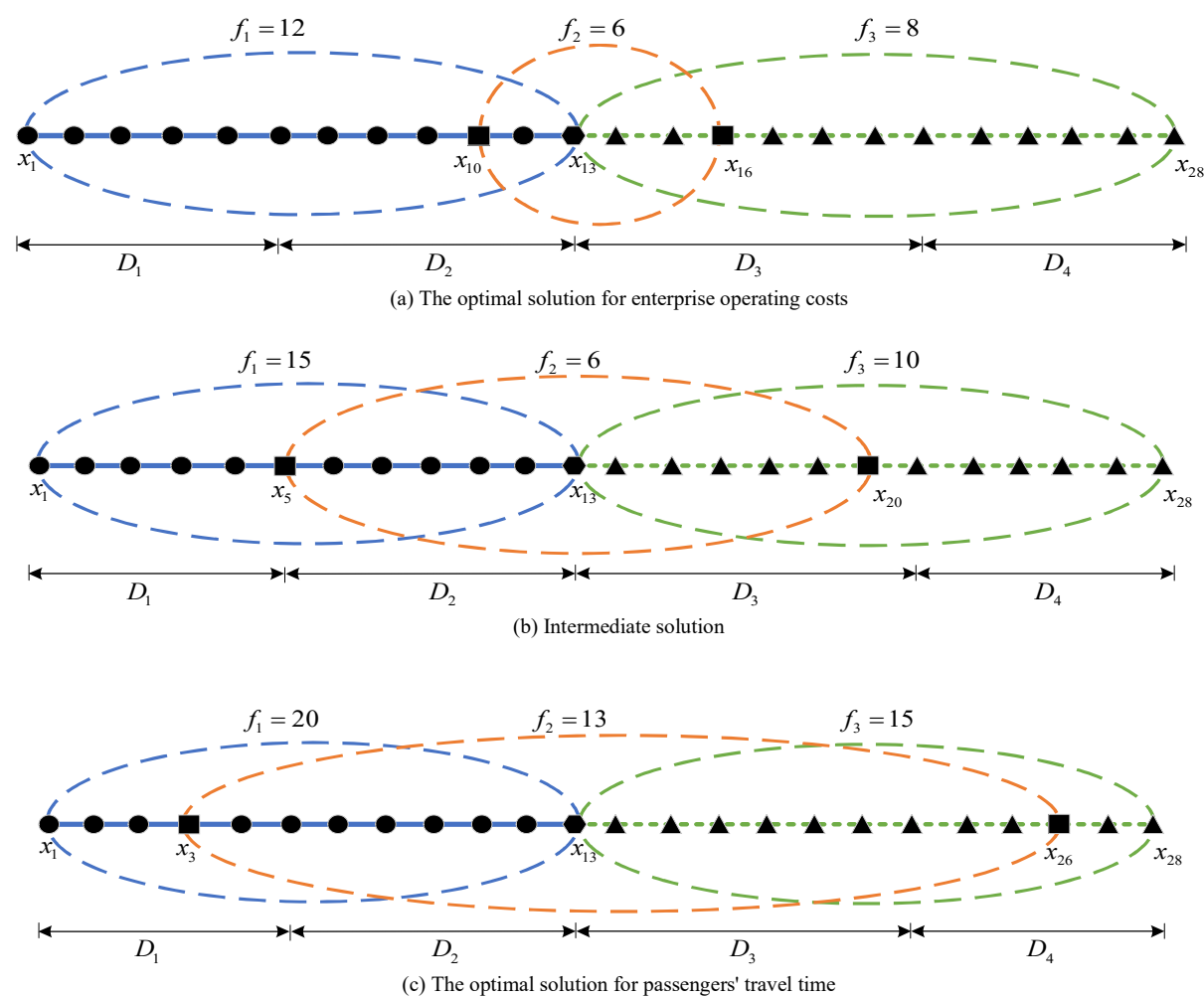


Fig.14. The optimized train operation plan

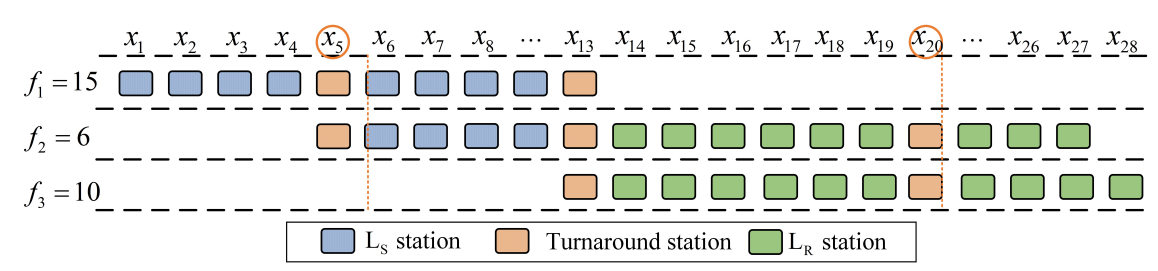


Fig.15. Optimized Train Operation Plan

As shown in Fig. 14(a), the "optimal solution for enterprise operating costs" maximizes cost savings. This is achieved by reducing the operating frequencies of all three train types. It also shortens the cross-line section distance and decreases the number of cross-line train pairs. These measures are taken while ensuring a basic service level. However, this solution exhibited issues such as excessively low passenger service levels and poor passenger comfort. Under the cross-line operation mode, passenger travel distance is lengthened. Passenger comfort significantly impacts satisfaction. Clearly, this solution is only suitable for a transitional phase. This phase occurs when vehicle equipment and facilities are not yet fully equipped. It also applies when the organizational methods for cross-line operation are not yet mature.

Fig. 14(b) illustrates the "intermediate solution." This solution is feasible. It maintains a certain service level while minimizing enterprise operating costs and passenger travel

time as much as possible. It achieves a balance between minimizing total passenger travel time and total enterprise cost.

Fig. 14(c) presents the "optimal solution for passenger total travel time." This solution aims to maximize passenger benefits. It is based on passenger preference for taking cross-line trains. It primarily reduces total passenger travel time. This reduction is achieved mainly by increasing the departure frequency of cross-line trains. Passenger ride comfort is also enhanced. However, this solution requires a large number of operational vehicles. Vehicle procurement costs are high. Line capacity for regional trains becomes constrained.

Under unchanged passenger flow and other parameters during peak hours, Line  $L_{\rm S}$  operated at a frequency of 17 pairs/h pairs/h under the transfer connection mode. Line  $L_{\rm R}$ 

operated at 12 pairs/h. The operation plans under the transfer connection mode and the cross-line operation mode were compared. A comparison of operation plans under these two modes is presented in Table 3.

TABLE III

COMPARISON OF OPERATION PLANS UNDER TWO OPERATING MODES

operation scheme	Z2/min	Relative savings	Z1/yuan	Relative savings
Transfer connection	264691.76	-	390498.06	-
Cross line operation	83131.51	70.00%	129345.34	66.87%

Table 3 shows that compared to the transfer connection mode, the cross-line operation mode saved 70.00% for Z1 and 66.87% for Z2. This indicates the effectiveness of the cross-line operation plan. It effectively optimizes both passenger travel time and enterprise operating costs.

To analyze the impact of the two operation modes on passenger travel time, the average travel times were compared. Comparisons were made for urban rail mainline passenger flow, suburban mainline passenger flow, and cross-line passenger flow. The comparison of average travel times for different passenger flow types is shown in Fig.16.

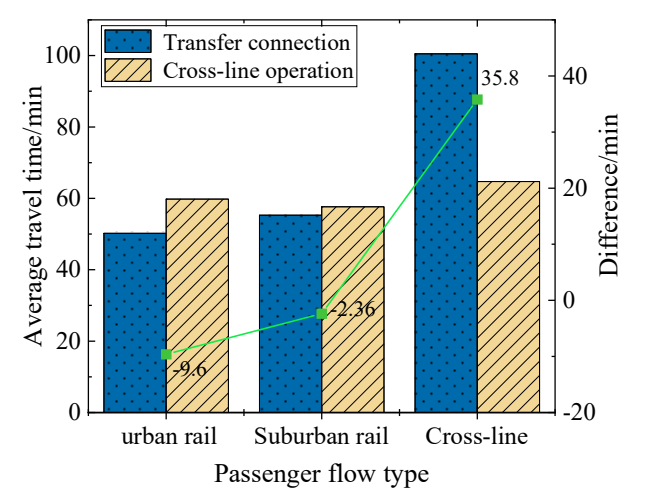


Fig.16. Comparison of average travel time for different types of passenger flow

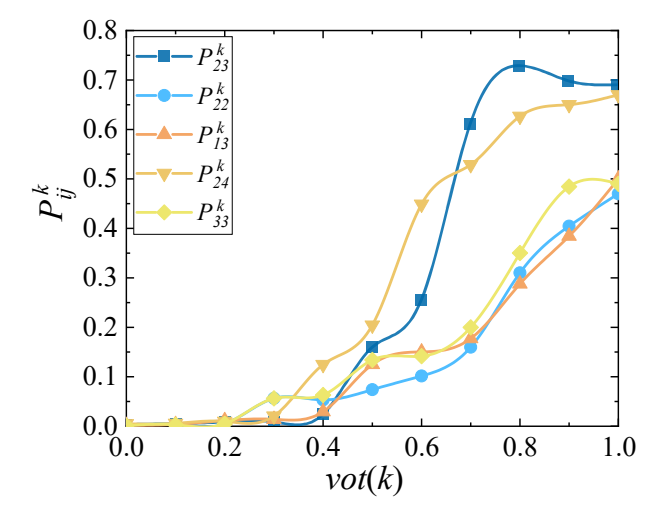
Fig.16. reveals that compared to the transfer connection mode, cross-line passenger flow travel time shortened under cross-line operation. The average saving was approximately 35.8 minutes. However, the average travel time increased for urban rail mainline passenger flow. It increased by 9.6 minutes. The average travel time also increased for suburban mainline passenger flow. It increased by 2.36 minutes. This indicates that cross-line operation can reduce travel time for cross-line passenger flow. However, it also leads to an increase in travel time for some local passenger flow. This increase is due to the reallocation of line resources. Therefore, actual operations should analyze passenger flow demand as

needed. Line resources should be allocated reasonably. This ensures an overall improvement in transportation efficiency.

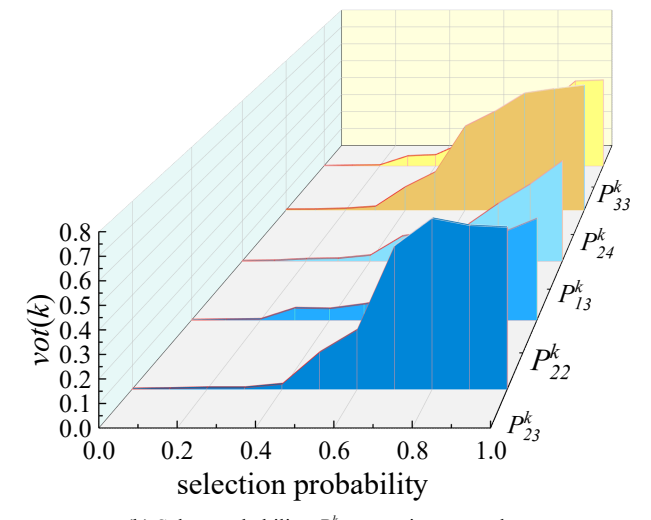
## B. Parameter analysis

(1) Influence of vot(h) on Passenger Choice Probability  $P_{ii}^{h}$ 

The complex mechanism between passenger time value and choice probability was explored. Taking the time value vot(k) of passengers choosing cross-line trains as an example, the variation of  $P_{ij}^k$  under different values of vot(k) was analyzed. The influence of time value on passenger choice probability is shown in Fig.17.



(a) The  $P_{ij}^{k}$  impact curve of vot(k) on



(b) Select probability  $P_{ij}^k$  comparison area chart

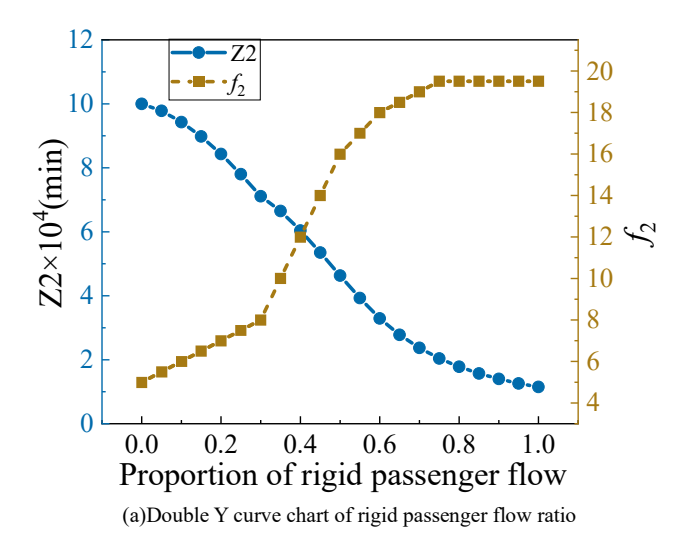
Fig.17. The Influence of Time Value on Passenger Choice Probability

Fig.17. shows that the probability of passengers choosing cross-line trains is positively correlated with time value vot(k). When vot(k) > 0.5, the probability reached its peak for passenger flows  $[D_2, D_3]$  and  $[D_2, D_4]$  choosing cross-line trains. This indicates their most urgent demand for cross-line trains. Consequently, operating cross-line trains is highly necessary when vot(k) > 0.5 and significant cross-track passenger flow exists. When  $vot(k) \le 0.5$ , the

probability of passengers choosing cross-line trains is relatively low. The demand for operating cross-line trains is also relatively small. In summary, operating cross-line trains can effectively meet passenger travel demands when passenger time value is high. It also improves transportation efficiency. In actual rail transit operation, cross-line train operation plans should be formulated reasonably. This should be based on passenger time value and passenger flow characteristics. The goal is to maximize operational benefits.

# (2) Influence of Rigid Passenger Flow Proportion on Operation Plan

The proportion of rigid passenger flow was adjusted in steps of 0.1. The intrinsic relationship between this proportion and total passenger travel time Z2 was systematically analyzed. The relationship with cross-line train departure frequency  $f_2$  was also analyzed. The influence of rigid passenger flow proportion on Z2 and  $f_2$  is shown in Fig.18.



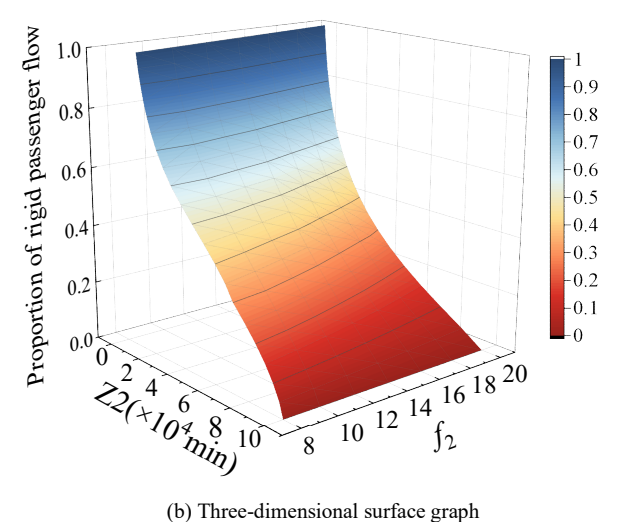


Fig.18. The impact of rigid passenger flow ratio on Z2 and  $f_2$ 

Fig.18 shows that as the proportion of rigid travel passenger flow increases, total passenger travel time Z2 gradually decreases. In contrast,  $f_2$  exhibits a nonlinear

characteristic. It first rises rapidly and then stabilizes. However, when the ratio exceeds 0.6, the marginal benefit of  $f_2$  weakens. This weakening is due to constraints in line capacity and vehicle operation capacity. Therefore, the proportion of rigid travel passenger flow directly affects the departure frequency  $f_2$  of cross-line trains. Planning the departure frequency of cross-line trains reasonably based on passenger travel demand is key. It is key to optimizing passenger travel time.

## (3) Fairness Analysis of Cross-line Operation

The impact of operating cross-line trains on resource allocation under cross-line operation was analyzed. The travel time change  $\mathfrak O$  was defined as passenger travel time under the traditional transfer mode minus that under cross-line operation.  $\mathfrak O$  positive  $\mathfrak O$  indicates time savings from cross-line operation. A negative  $\mathfrak O$  indicates time loss caused by cross-line operation. The travel time change  $\mathfrak O$  for different passenger types in different travel zones was analyzed separately. Changes in travel time for different passenger flows in different zones are shown in Fig.19.

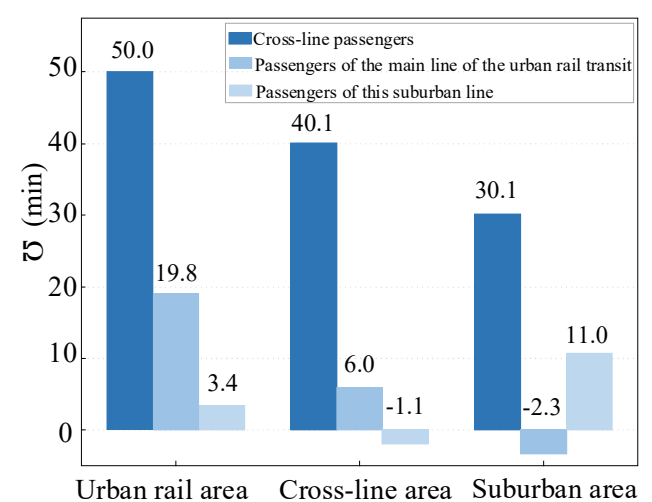


Fig.19. shows the changes in travel time of different passenger flows in different regions

As shown in Fig.19, cross-line passenger flow experiences the most travel time savings due to cross-line operation, regardless of whether they are in the urban rail zone, cross-line zone, or suburban zone. Therefore, cross-line operation has a direct advantage, reducing transfer time, waiting time, etc., for passengers compared to the traditional transfer mode. Operating cross-line trains provides significant advantages for cross-line passenger flow. However, for urban rail local passenger flow, travel time to suburban areas increased by 2.3 minutes after operating cross-line trains. For suburban local passenger flow, travel time to cross-line areas increased by 1.1 minute. Therefore, a resource competition relationship exists between cross-line trains and local trains. Operating cross-line trains occupies resources originally allocated to local trains, leading to increased travel time for some local passenger flow.

To further analyze the fairness of cross-line operation, the Lorenz curve is used to calculate the Gini coefficient to measure the unfairness degree of passenger travel time changes. The cumulative proportion of time savings for each passenger under the cross-line operation mode is calculated. The Lorenz curve is shown in Fig.20.

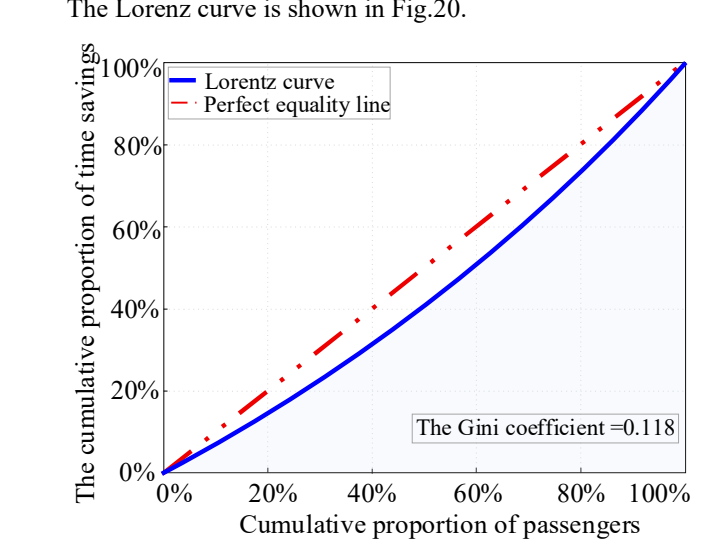


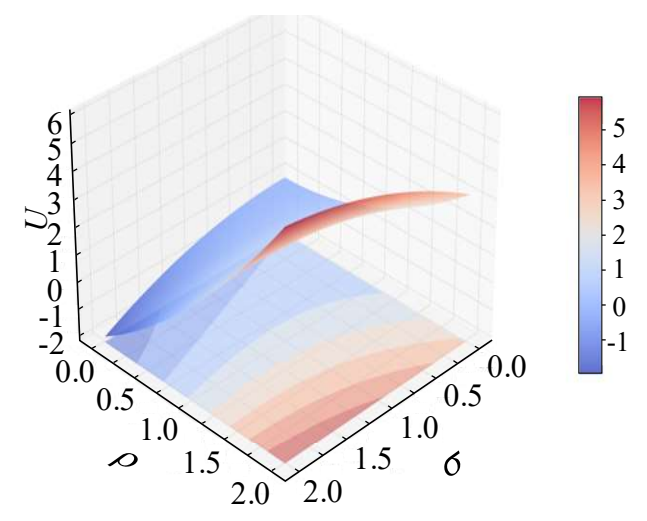
Fig.20. Shows the changes in travel time of different passenger flows in different regions

Fig.20 shows that the curve approaches 100% on the vertical axis at the 60% point on the horizontal axis. This indicates that time savings are highly concentrated among cross-line passenger flow. It also explains the curve's rapid rise. Meanwhile, the Gini coefficient is 0.118. This is far below the international warning line of 0.4. It indicates a balanced distribution of passenger time savings/losses under cross-line operation. Combined with Fig. 19, cross-line operation increases travel time for some local passenger flow. Overall, however, by reasonably distributing travel time losses and gains among passengers, serious unfairness in travel time between passenger flows is avoided.

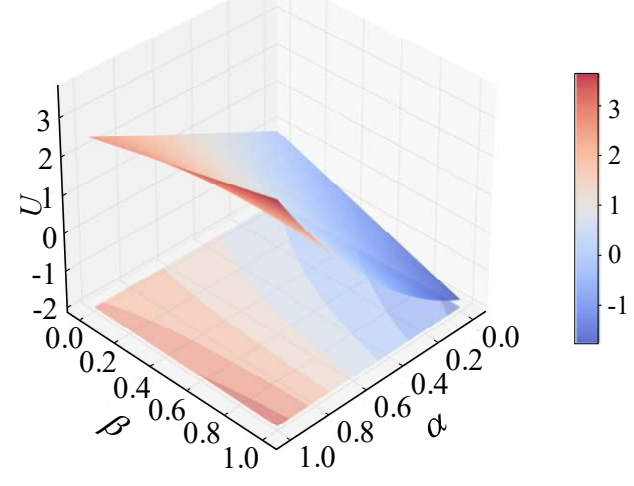
## (4) The Impact of MA-CPT Model Parameters on Cumulative Prospect Value U

The impact of the gain sensitivity coefficient, loss sensitivity coefficient, discrimination coefficient, and attractiveness coefficient on the comprehensive travel utility U is analyzed separately. The impact of MA-CPT model parameters on U is shown in Fig.21.

As seen from Fig.21, the cumulative prospect value U increases with the increase of  $\alpha$  and  $\beta.$  At the same time, it can be seen that the gain sensitivity coefficient  $\alpha$  has a greater influence on the cumulative prospect value than the loss sensitivity coefficient  $\beta.$  This indicates that when the route travel time is less than the passenger's expectation, passengers tend to have a risk-averse mentality. Meanwhile, the cumulative prospect value U increases with the increase of  $\sigma,$  but decreases with the increase of  $\rho.$  It is evident that the discrimination parameter  $\sigma$  has a far greater impact on the cumulative prospect value than the attractiveness parameter



(a) The influence of the discrimination coefficient and the attraction parameter on  ${\cal U}$ 



(b) The influence of the gain sensitivity coefficient and the loss sensitivity coefficient on  ${\cal U}$ 

Fig.21. The influence of NL-MA-CPT model parameters on travel utility

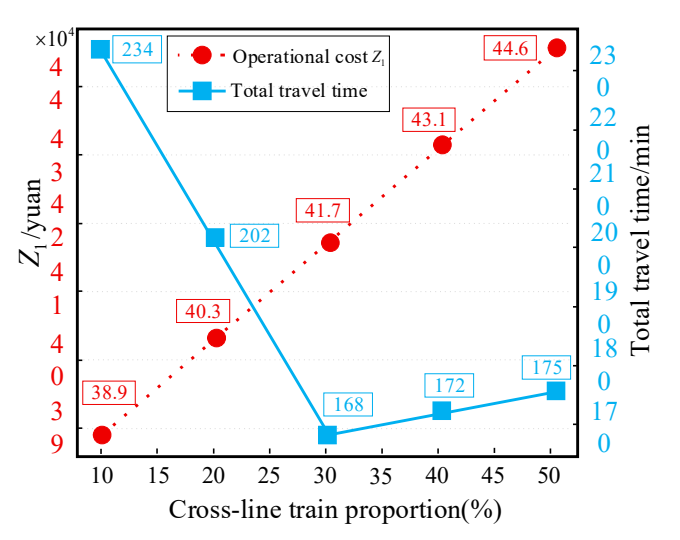
Therefore, passengers pay more attention to "gaining time savings" than "avoiding losses," reflecting a gain preference orientation in decision-making. When optimizing services, it is necessary to focus on meeting the timeliness demands of high- $\alpha$  passengers (such as business commuters). Shortening waiting/transfer times can significantly improve their satisfaction. At the same time, passengers pay more attention to the actual travel time than psychological expectations. Operational strategies should focus on optimizing actual timeliness rather than psychological anchoring.

## (4) Impact Analysis of Cross-line Train Proportion

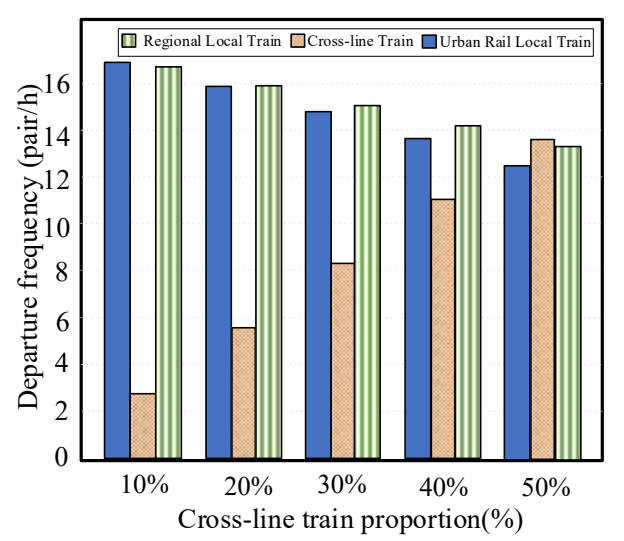
To optimize the allocation of rail transit network resources while achieving the optimal balance between operational costs and service quality in meeting passenger travel demands, this study analyzes the impact of cross-line train operation frequency on both passenger travel time and enterprise operational costs.

As seen from Fig.22. The line chart reveals a nonlinear relationship between cross-line train proportion and both operational costs  $(Z_1)$  and passenger travel time  $(Z_2)$ . The

operational cost exhibits a monotonically increasing trend, rising from 389,000 CNY at 10% proportion to 446,000 CNY at 30%, after which it stabilizes. This indicates that increasing the cross-line train proportion incurs additional operational costs, with saturation occurring beyond 30%. In contrast, passenger travel time follows a more complex U-shaped curve. It decreases significantly from 234 minutes at 10% to 168 minutes at 25% (a 28.2% reduction), then slightly rebounds to 172 minutes at 30%, and ultimately reaches 175 minutes at 50%. This pattern suggests an optimal cross-line train proportion range (20%-30%) where passenger travel time is minimized.



(a) Impact of Cross-line Train Proportion on Operational Cost and Passenger
Travel Time



(b) Departure Frequency Distribution of Different Train Types under Varying Cross-line Proportions

Fig.22. Departure Frequency Distribution of Different Train Types under Varying Cross-line Proportions

The departure frequency distribution illustrates the dynamic scheduling strategy for different train types under varying cross-line train proportions. The frequency of regional local trains first decreases from 16 pair/h at 10% to 10 pair/h at 40%, then rebounds to 14 pair/h at 50%,

reflecting adaptive resource allocation across operational modes. The cross-line train frequency generally increases from 8 pair/h at 10% to 14 pair/h at 30%, but experiences an anomalous drop to 10 pair/h at 40%, likely due to line capacity constraints. Meanwhile, the urban rail local train frequency remains stable at 12-14 pair/h, reinforcing its role as a foundational service.

The two charts collectively validate the existence of an optimal cross-line train proportion range (20%-30%). Within this range, the system achieves minimized passenger travel time (~168-172 minutes) while maintaining acceptable operational costs (~417,000-446,000 CNY), aligning with the paper's core argument on the "optimal balance in resource allocation." The frequency adjustment strategy further demonstrates the model's intelligence. By dynamically reallocating regional local train resources to accommodate cross-line train demand while preserving urban rail service stability, the system optimizes overall efficiency. Notably, at 30% cross-line train proportion, a balanced frequency distribution (regional local: 12 pair/h; cross-line: 14 pair/h; urban rail: 12 pair/h) coincides with near-minimal travel time, confirming the model's scheduling efficacy. Beyond 30%, despite higher cross-line train frequencies, passenger travel time shows no further improvement and even slightly deteriorates, while operational costs remain elevated. This phenomenon supports the paper's thesis on "diminishing marginal returns of cross-line train services," providing quantitative guidance for practical proportion-setting in operations.

## VI. CONCLUSION

- 1) This study proposes the innovative application of the NL-MA-CPT theory to multi-level rail transit cross-line operation research. We developed an optimization model for cross-line train operation plans that integrates passengers' multi-attribute choice behaviors. The model reveals the complex mechanism of passenger flow allocation and operational resource coordination under bounded rationality. It provides a theoretical foundation for the collaborative optimization of multi-level rail networks. In practical applications, model parameters should be dynamically adjusted based on specific line characteristics to enhance adaptability.
- 2) Compared to the transfer connection mode, the cross-line operation mode significantly reduces the average travel time for cross-line passenger flow by 35.8 minutes. It also lowers the total passenger travel time by 70.00% and reduces enterprise operating costs by 66.87%.
- 3) The probability of passengers choosing cross-line trains is positively correlated with their value of time, with high time-value passenger groups exhibiting particularly strong demand for direct services. When the cross-line train

operation proportion reaches 30% (corresponding to 12 trains/h for regional local trains, 14 trains/h for cross-line trains, and 12 trains/h for urban rail trains), passenger travel time approaches its optimal level. Beyond this threshold, further increases in cross-line services lead to diminishing marginal returns-travel time ceases to improve and may even deteriorate slightly, while operational costs continue to rise. Concurrently, when the proportion of rigid demand exceeds 0.6, the marginal benefits of increasing cross-line train frequency diminish significantly due to line capacity constraints. Consequently, priority should be given to augmenting cross-line train frequency during rigid demand-dominated periods, whereas frequency may be moderately reduced in flexible demand scenarios to optimize costs. Equity analysis demonstrates that while cross-line operations may marginally increase travel time for some local passengers, the overall distribution of time savings and losses across passenger groups remains balanced, effectively preventing significant inequities.

4) Future research should focus on incorporating real-time passenger flow data. Building a time-varying parameter framework will enhance the adaptability of operation plans to sudden demand fluctuations. Exploring collaborative scheduling mechanisms between cross-line operation and other transportation modes could further improve the resilience of regional transportation networks.

#### REFERENCES

- C. Zhu, X. Yang, Z. Wang, J. Fang, J. Wang, and L. Cheng, "Optimization for the train plan with flexible train composition considering carbon emission," Engineering Letters, vol. 31, no. 2, pp. 562-573, 2023.
- [2] H. Wu, J. Zhen, and J. Zhang, "Urban rail transit operation safety evaluation based on an improved CRITIC method and cloud model," Journal of Rail Transport Planning & Management, vol. 16, Article ID 100206, 2020.
- [3] M. Ito, "Through service between railway operators in Greater Tokyo," Japan Railway & Transport Review, vol. 63, pp. 14-21, 2014.
- [4] J. W. Vigrass, "Alternative forms of motive power for suburban rail rapid transit," in ASME/IEEE Joint Conference on Railroads, pp. 65-77, 1990.
- [5] G. Drechsler, "Light railway on conventional railway tracks in Karlsruhe, Germany," in Proceedings of the Institution of Civil Engineers-Transport, vol. 117, no. 2, pp. 81-87, 1996.
- [6] L. Sato and P. Essig, "How Tokyo's Subways Inspired the Paris RER," Japan Railway & Transport Review, vol. 23, pp. 36-42, 2000.
- [7] M. Novales, A. Orro, and M. Bugarin, "Madrid tram-train feasibility study conclusions," in Proceedings of the Institution of Mechanical Engineers, Part F: Journal of Rail and Rapid Transit, vol. 217, no. 1, pp. 1-10, 2003.
- [8] L. Tang and X. Xu, "Optimization for operation scheme of express and local trains in suburban rail transit lines based on station classification and bi-level programming," Journal of Rail Transport Planning & Management, vol. 21, Article ID 100283, 2022.
- [9] L. Tang, A. D'Ariano, X. Xu, et al., "Scheduling local and express trains in suburban rail transit lines: Mixed-integer nonlinear programming and adaptive genetic algorithm," Computers & Operations Research, vol. 135, Article ID 105436, 2021.
- [10] J. Parbo, O. A. Nielsen, and C. Prato, "Reducing passengers' travel time by optimizing stopping patterns in a large-scale network: A case-study in the Copenhagen Region," Transportation Research Part A: Policy and Practice, vol. 113, pp. 197-212, 2018.

- [11] E. Altazin, S. Dauzère-Pérès, F. Ramond, et al., "Rescheduling through stop-skipping in dense railway systems," Transportation Research Part C: Emerging Technologies, vol. 79, pp. 73-84, 2017.
- [12] P. Shang, R. Li, Z. Liu, et al., "Timetable synchronization and optimization considering time-dependent passenger demand in an urban subway network," Transportation Research Record, vol. 2672, no. 8, pp. 243-254, 2018.
- [13] A. Yang, B. Wang, and J. Huang, "Service replanning in urban rail transit networks: Cross-line express trains for reducing the number of passenger transfers and travel time," Transportation Research Part C: Emerging Technologies, vol. 115, Article ID 102629, 2020.
- [14] A. Yang, J. Huang, B. Wang, et al., "Train scheduling for minimizing the total travel time with a skip-stop operation in urban rail transit," IEEE Access, vol. 7, pp. 81956-81968, 2019.
- [15] L. Tang and X. Xu, "Optimization for operation scheme of express and local trains in suburban rail transit lines based on station classification and bi-level programming," Journal of Rail Transport Planning & Management, vol. 21, Article ID 100283, 2022.
- [16] Z. Li, B. Mao, Y. Bai, et al., "Integrated optimization of train stop planning and scheduling on metro lines with express/local mode," IEEE Access, vol. 7, pp. 88534-88546, 2019.
- [17] Z. Chen, S. Li, A. D'Ariano, et al., "Real-time optimization for train regulation and stop-skipping adjustment strategy of urban rail transit lines," Omega, vol. 110, Article ID 102631, 2022.
- [18] J. Shao, Y. Xu, L. Sun, et al., "Equity-oriented integrated optimization of train timetable and stop plans for suburban railways system," Computers & Industrial Engineering, vol. 173, Article ID 108721, 2022.
- [19] T. Zhu, Y. Su, and T. Huang, "A dimension reduction classification method combining chaotic mapping and genetic algorithm for Zhuhai-1 hyperspectral images," in International Conference on Wireless Communications, Networking and Applications, pp. 384-389, 2022.
- [20] H. Lu, R. Niu, J. Liu, and Z. Zhu, "A chaotic non-dominated sorting genetic algorithm for the multi-objective automatic test task scheduling problem," Applied Soft Computing, vol. 13, no. 5, pp. 2790-2802, 2013
- [21] C. Jiao, K. Yu, and Q. Zhou, "An opposition-based learning adaptive chaotic particle swarm optimization algorithm," Journal of Bionic Engineering, vol. 21, pp. 3076–3097, 2024.
- [22] Y. Zhan, M. Ye, R. Zhang, S. He, and S. Ni, "Multi-objective optimization for through train service integrating train operation plan and type selection," Transportation Letters, vol. 16, no. 9, pp. 1039-1058, 2024.
- [23] L. Kang, Y. Lai, J. Wang, and W. Cao, "A Pacesetter-Lévy multi-objective particle swarm optimization with Arnold Chaotic Map with opposition-based learning," Information Sciences, vol. 678, pp. 121048, 2024.
- [24] X. Di and H. X. Liu, "Boundedly rational route choice behavior: A review of models and methodologies," Transportation Research Part B: Methodological, vol. 85, pp. 142-179, 2016.



Shuoyue Gao was born in Shaanxi, China. She received her Bachelor's degree in Traffic and Transportation from Shijiazhuang Tiedao University, China, in 2023. Currently, she is pursuing a Master's degree in Traffic and Transportation (Railway Transportation Engineering) at Lanzhou Jiaotong University. Her research interests include through operations and passenger flow distribution.